Stoch Environ Res Risk Assess (2013) 27:1221–1230
DOI 10.1007/s00477-012-0658-x

ORIGINAL PAPER

Phase difference analysis of temperature and vegetation phenology for beech forest: a wavelet approach

Gudrun Carl · Daniel Doktor · Dirk Koslowsky · Ingolf Kühn

Published online: 3 November 2012

Abstract Temporal shifts in phenology or vegetation period of plants are seen as indicators of global warming with potentially severe impacts on ecosystem functioning. In spite of increasing knowledge on drivers, it is of utmost importance to disentangle the relationship between air temperatures, phenological events, potential temporal lags (phase shifts) and time scale for certain plant species. Assessing the phase shifts as well as the scale-dependent relationship between temperature and vegetation phenology requires the development of a nonlinear temporal model. Therefore, we use wavelet analysis and present a framework for identifying scale-dependent cross-phase coupling of bivariate time series. It allows the calculation of (a) scale-dependent decompositions of time series, (b) phase shifts of seasonal components in relation to the annual cycle, and (c) inter-annual phase differences between seasonal phases of different time series. The model is applied to air temperature data and remote sensing phenology data of a beech forest in Germany. Our study reveals that certain seasonal changes in amplitude and phase with respect to the normal annual rhythm of temperature and beech phenology are coupled time-delayed components, which are characterized by a time shift of about one year.

Keywords Beech forest · Bivariate time series analysis · Coherence phase · Morlet wavelet · Normalized difference vegetation index · Remote sensing signal

G. Carl (✉) · I. Kühn
Department of Community Ecology, UFZ—Helmholtz Centre for Environmental Research, Theodor-Lieser-Str. 4, 06120 Halle, Germany
e-mail: gudrun.carl@ufz.de

D. Doktor
Department of Computational Landscape Ecology, UFZ—Helmholtz Centre for Environmental Research, Permoserstr. 15, 04318 Leipzig, Germany

D. Koslowsky
Department of Meteorology, Free University of Berlin, Carl-Heinrich-Becker-Weg 6-10, 12165 Berlin, Germany

1 Introduction

Time shifts in the phenology of plant species (e.g. earlier onset of flowering, early start and prolonged duration of vegetation period) are seen as indicators of global warming (Badeck et al. 2004; Post et al. 2008). In particular, changes in flowering phenology such as date of first flowering can be a response to climate change. Although plant phenology depends on various climate variables, temperature is the main driver for many species (Badeck et al. 2004; Cleland et al. 2007; Delbart et al. 2008; Menzel 2000). It was found that the onset of flowering is correlated with the mean temperature of the flowering month or the months prior to flowering (Menzel et al. 2006; Sparks et al. 2000). Responding to recent warming, many plants are flowering earlier in most study areas today (Menzel 2003; Miller-Rushing et al. 2008; Parmesan 2007). Especially in temperate and boreal systems, the initiation of spring activity is mainly driven by an immediately antecedent period of sufficiently high temperatures for many species (Badeck et al. 2004). For some species, such as beech (*Fagus sylvatica*), however, it was stated long ago that bud burst is strongly dependent on day length (Wareing 1953) rather than chilling or temperature requirements. Therefore one can expect that the dependence on day-length could

counteract physiological responses to altered climatic regimes.

In spite of such increasing knowledge, it is crucial to take into account that phenological events depend on plant species and scale. Temporal shifts in phenology can be the result of shifts in the temperature regime. However, it may occur for different species on different temporal scales. Moreover, vegetation phenology may not be exclusively driven by immediately antecedent temperatures. Modeling the impact of climatic parameters such as temperature on the phenology of certain species across different seasons and temporal scales is therefore a prerequisite for understanding the species–climate relationship. It is of utmost importance to disentangle the relationship between air temperature, phenological events, and scale for certain plant species.

Various studies analyzed the effects of temperature on the phenological timing of plants. For an overview, see Lu et al. (2006). In general, the authors analyzed phenological ground observations in relation to mean monthly air temperatures or mean temperatures of a period of several months. For example, Chmielewski and Rötzer (2001) calculated linear regressions concerning the influence of air temperature. In particular, the annual lengths of growing season are regressed on the mean annual air temperatures. Lu et al. (2006) demonstrated the need for a better understanding, refined the method and used average temperatures over different periods to calculate the correlation of temperature with flowering dates. Hudson (2010) explored recent and newly developed analytic and statistical methods in vegetation phenology.

In the presence of strong scale-dependence, a linear approach will not be able to extract information on when coupling between environmental factors such as temperature and species phenology occurs. Instead, scale-dependent analyses of coupling between two time series would be needed for a systematic investigation of periods when temperature has a potential influence on plant growing. Wavelet analysis has been proved to be a suitable mean to quantify temporal structure as a function of both time and scale (Percival and Walden 2000). Many of the concepts for wavelet analysis apply to time series analysis. Because wavelet analysis does not assume stationarity of the process creating the data, it is a more general approach than common analysis techniques such as Fourier analysis. Wavelet transform is a powerful method to reveal and identify time periods of the frequency-dependent variations in a time series (Yang et al. 2010). The technique has proved especially valuable, e.g., in hydrological applications such as tidal analysis and analysis of high/low water levels at rivers (Zhang et al. 2010). Therefore, an analysis based on wavelets should also be a suitable method to solve the problems posed above.

However, wavelet analysis is an apparently little-known method in the field of phenology (Hudson 2010). Using satellite data for vegetation phenology in combination with different wavelet techniques, the authors pursue different strategies. White et al. (2003) firstly determined start and end of a growing season at different sites. Afterwards, they used wavelet variance analysis to analyze spatial patterns and dominant scales of such growing season lengths. In a different way, the same topic is addressed by Yang et al. (2012). Using scale-dependent wavelet decomposition, they firstly extracted several important features characterizing vegetation dynamics. Thereafter they discussed spatial patterns and correlations between these key features and climatic factors. In a third manner, Hudson et al. (2011) applied wavelet transforms in phenological research. To improve the understanding of flowering–climate relationship, they evaluated wavelet cross-correlations of bivariate time series. This was achievable because, for eucalypt species, the authors were able to utilize phenological records that, although originating from traditional land based phenology, are characterized by relatively high information content. However, they used discrete wavelet transforms, which are limited to a discrete set of scales.

In a similar way, the focus in our study will be on bivariate time series analysis and detecting couplings between two series. A good introduction to wavelet methods for time series analysis was given by Percival et al. (2004). Calculations of wavelet power spectra characterized by an arbitrary fine set of scales can be carried out by continuous non-orthogonal wavelet transforms (Torrence and Compo 1998). Cross-wavelet spectra have been used to identify both frequency bands and time intervals within which two different time series are covarying. For complex-valued wavelet functions, it is additionally possible to calculate phases. Therefore, such wavelets are particularly suitable for capturing oscillatory behavior (Torrence and Compo 1998). Phase differences between two time series can be calculated by the coherence phase. Such wavelet methods have been successfully applied in geophysics and climatology. For example, links between temperature or rainfall and North Atlantic oscillation index or El Niño–southern oscillation index were investigated (Torrence and Webster 1999; Paluš et al. 2005). Afterwards, phase analysis concepts based on continuous wavelet transforms were adopted and applied in the fields of medicine (Cazelles et al. 2005; Grenfell et al. 2001) and ecology and population biology (Klvana et al. 2004; Cazelles et al. 2008). In the papers in biology, the authors analyzed the possible association between the cycles of population abundance of some animals and environmental signals such temperature, precipitation, and the solar cycle.

The focus in our study will be on phenological data derived from satellite observations, its seasonal and interannual variability, and the bivariate relationship between phenological and temperature time series. To address the

issue of periods when temperature has a potential influence on plant growing, seasonal fluctuations in relation to the normal annual rhythm must be taken into account regarding their influence on the vegetation phenology, i.e. timing and phase of plant development. Therefore, the main objective of this paper is to analyze the scale-dependent coupling of phenological and temperature data. By applying the techniques of wavelet analysis, we will be able to determine to which extent the phase shifts are dependent on scale. Furthermore, the methodology presented below allows us to detect scale-dependent inter-annual phase shifts. The model is applied to daily air temperature data and daily NDVI (normalized difference vegetation index) observations (Doktor et al. 2009) of a beech forest in Germany.

2 Methods

2.1 Morlet wavelets

A complex-valued wavelet for a complex continuous wavelet transform is required for our application, as it yields information on both the amplitude and the phase of time series without any restrictions on scale. There are a few different types of complex-valued wavelets. The advantage of the Morlet wavelet is that it has optimal joint time–frequency concentration with respect to the Heisenberg's uncertainty principle, i.e. it attains the minimum possible value regarding time–frequency–resolution (Aguiar-Conraria et al. 2008). Therefore, the use of Morlet wavelets is especially advantageous in case of insufficient prior knowledge of phase and frequency variations.

The Morlet wavelet including its family of scaled and translated versions is given by

$$\Psi_{\tau,f}(t) = \pi^{-1/4} s^{-1/2} \cdot \exp[2\pi i f(t-\tau)] \cdot \exp\left[-\frac{(t-\tau)^2}{2s^2}\right]$$

for different scale and location parameters f and τ, respectively. These complex-valued Morlet wavelets are products of a complex exponential of frequency f and a Gaussian density function. This Gaussian is centred at time τ and characterized by a width s (or standard deviation s as well-defined parameter in a statistical context), which is approximately proportional to the inverse of f (Lachaux et al. 2000; Foufoula-Georgiou and Kumar 1997). Therefore, the real and imaginary parts of the wavelets are sinusoidal waves modulated by a Gaussian function. The wavelet transform of function $x(t)$ at time τ and frequency f is defined as

$$W_x(\tau,f) = \int_{-\infty}^{\infty} x(t) \cdot \Psi^*_{\tau,f}(t)dt$$

where $\Psi^*_{\tau,f}$ is the complex conjugate of the Morlet wavelet. Because $W_x(\tau,f)$ is complex as well, it is an expression of the form

$$\begin{aligned} W_x(\tau,f) &= Re\{W_x(\tau,f)\} + iIm\{W_x(\tau,f)\} \\ &= |W_x(\tau,f)| \exp[i\Phi(\tau,f)] \end{aligned} \quad (1)$$

where real and imaginary part are denoted $Re\{W_x(\tau,f)\}$ and $Im\{W_x(\tau,f)\}$, respectively. Using Morlet wavelets, one is able to estimate the instantaneous amplitude

$$|W_x(\tau,f)| = \sqrt{\left[Re\{W_x(\tau,f)\}\right]^2 + \left[Im\{W_x(\tau,f)\}\right]^2} \quad (2)$$

and the instantaneous phase of the signal (Torrence and Compo 1998).

$$\Phi_x(\tau,f) = \text{atan2}[Im\{W_x(\tau,f)\}, Re\{W_x(\tau,f)\}] \quad (3)$$

where atan2 is the two-argument inverse tangent. If the function that should be analysed is a nearly periodic function representable by $x(t) = A(t)\cos[2\pi f_0 t + \varphi_x(t)]$, then this instantaneous phase measures the shift between function $x(t)$ and sinusoidal wave $Re\{exp[-2\pi i f(t-\tau)]\} = \cos[2\pi f(t-\tau)]$ for different scale and location parameters f, τ. Hence it follows for $f_0 = f$, that the effective phase is

$$\tilde{\varphi}_x = \Phi_x - 2\pi f \tau. \quad (4)$$

In order to avoid large increases of phase values, the last step in phase calculation is the transformation from effective phase to wrapped effective phase, i.e. a phase constrained to an interval such as $[0, 2\pi)$:

$$\varphi_x = \tilde{\varphi}_x \ mod\ 2\pi. \quad (5)$$

Given two time series $x(t)$ and $y(t)$ with wavelet transforms $W_x(\tau,f)$ and $W_y(\tau,f)$, respectively, the cross-wavelet transform is defined as $W_{xy}(\tau,f) = W_x(\tau,f)W^*_y(\tau,f)$ and the coherence phase as

$$\Phi_{xy}(\tau,f) = \text{atan2}\left[Im\{W_{xy}(\tau,f)\}, Re\{W_{xy}(\tau,f)\}\right] \quad (6)$$

(Torrence and Compo 1998).

2.2 Wavelet analysis

In the following, we consider in more detail how wavelet transforms can be used to study the issue of periods when temperature has a potential influence on plant growing.

As a starting point for subsequent analysis, all series were normalized. The procedure itself includes the

following three steps: calculation of (1) scale-dependent decompositions of time series, (2) phase shifts of seasonal components in relation to the annual cycle, and (3) inter-annual phase differences between seasonal phases of different time series. This means in detail:

(1) The analysis is based on a previous time–frequency analysis of the time series. Because nearly periodic time series are characterized by a specific frequency they can be estimated by $\hat{x}(\tau,f) = |W_x(\tau,f)|\cos[2\pi f\tau + \varphi_x(\tau,f)]$, that is a sinusoidal oscillation as a function of time-dependent amplitudes [Eq. (1)–(2)] and phases [Eq. (3)–(5)] calculated by wavelet analysis (Paluš et al. 2005). Moreover, signals can be decomposed into a finite set of such frequency components. To correctly represent the dominant component of an annual cycle, one should regard the period length of the tropical year $T = 365.25\,d$ as lowest mode of oscillation. Thus the lowest frequency is one cycle per year. According to this fundamental frequency $f_0 = 1/T$, the harmonics should have frequencies $f_1 = 2f_0, f_2 = 4f_0, f_3 = 8f_0, \ldots$etc. This is feasible with Morlet wavelets, because in case of such continuous wavelet transforms not only several numbers of octaves (powers of 2), but also several scales per octave can be utilized for the adjustment of frequencies. The subsequent analysis is done on these frequency components $\hat{x}(\tau,f_i)$ of the signals.

(2) Here, we introduce our method of detecting fluctuations in the timing of the seasons. Phase analysis is able to reveal how the frequency components $\hat{x}(\tau,f_i)$ are phase-shifted in relation to a normal annual rhythm. Thus, in order to investigate seasonal dynamics, phases [Eq. (3)–(5)] have to be calculated, where x is to replace by $\hat{x}(\tau,f_i)$ and f is to replace by f_0. In this way, phase relations of frequency components $\hat{x}(\tau,f_i)$ to an annual cycle are calculated. More precisely, the calculated phase time series $\varphi_{\hat{x},f_i}(\tau,f_0)$ reflect the time-dependent forerun of the components $\hat{x}(\tau,f_i)$ to the function $\cos[2\pi f_0\tau]$. To exemplify and to realize what is meant for phases of functions at different frequencies, one can compare the positions of zeros. For $f_i = f_0$, every zero of the component $\hat{x}(\tau,f_0)$ is compared to every zero of the cosine. Whereas, for instance, for $f_i = f_1$, every second zero of the component $\hat{x}(\tau,f_1)$ is compared to every zero of the cosine. In a sense, the components $\hat{x}(\tau,f_i)$ are regarded as functions of frequency f_0, and additional zeros must be seen just as specific amplitudes rather than nodes of oscillation.

(3) Having such phases calculated for both time series, it is of particular interest whether a distinct temporal phase difference will become apparent in the process. Phase differences of two time series can be calculated by the coherence phase [Eq. (6)]. If the phase difference between two signals is constant over time, these signals can be regarded as phase-locked. Waves characterized by constant phase difference are referred to as coherent waves, and periods of constant phase difference are referred to as periods of synchronization (Cazelles and Stone 2003; Pikovsky et al. 2001). Long-term synchrony allows the assumption that both signals are coupled, i.e. one signal reacts to the other, possibly with a certain time lag. In order to detect scale-dependent and inter-annual phase shifts, we apply Eq. (6) to the seasonal phases $\varphi_{\hat{x},f_i}$ and $\varphi_{\hat{y},f_i}$ instead of x and y. In this case, we have to calculate this coherence phase for an appropriate low frequency, i.e. for a frequency lower than one cycle per year. Phase shift can always be converted into time shift. For this purpose, an appropriate frequency band has to be applied.

Our computations are based on a software package housed in the R language (R version 2.11.1) and environment for statistical computing (R Development Core Team 2010). The tools for calculating wavelet transforms are available in the package *dplR* (Bunn 2008). We used the function *morlet* for Morlet wavelets.

3 Data

Vegetation activity has been well documented using two independent methods for data collection, based on ground observations and remote sensing measurements. Remote sensing signals are satellite observations provided by, for instance, the National Oceanic and Atmospheric Administration's Advanced Very High Resolution Radiometer (NOAA/AVHRR). Signals observed by remote-sensing techniques are available as so-called normalized difference vegetation index (NDVI) values. This index exploits the change in reflectance between the red and infra-red part of the electromagnetic spectrum typically exhibited by vegetation. The NDVI thus reflects the part of photosynthetically relevant radiation absorbed by plants. Using remote-sensing indices, several authors were able to estimate the date of green-up or the length of vegetation period for, e.g., deciduous forests (Badeck et al. 2004; White et al. 2003). Roughly speaking, NDVI data reflect changes in leaf and shoot growth and indicate the seasonal greenness of the vegetation as seen from space.

NDVI values are available as daily signals in 1×1 km^2 spatial resolution for the period 1989–2007. In a systematic pre-processing of data, a general quality check is necessary to identify missing data, outliers, and other errors in data recording. Moreover, elimination from cloudy scenes and

of directional and atmospheric effects necessitates further corrections (Doktor et al. 2009). Therefore, a dynamic filtering of raw satellite data was used to improve the observational data. In the resulting dataset missing or faulty observations are replaced by linear interpolation between selected 'true' NDVI observations.

We focus on the seasonal activities of a temperate deciduous forest. Because it would be a disadvantage if a mixture of different species within the satellite scene has to be analyzed, we try to concentrate our study on a single species. This is possible for a large beech forest area consisting of nearly pure stands of beech (*Fagus sylvatica*). The selected observation area is a grid cell (upper left corner: 51°06′12″N, 10°22′35″E, altitude 445 m a.s.l.) of about 1 km^2 in a beech forest located in Germany (Hainich). The Hainich site is located in western Thuringia. It is a national park that has not been managed regularly for about 40 years. Since the forest was managed as coppice-with-standards forest or selection forest before (instead of age-class forest), only single trees were removed. Thus to date the stand has been uneven-aged with old dominant trees (Skomarkova et al. 2006).

Weather data are provided by the German Meteorological Service (DWD) for distributed stations (WebWerdis, http://werdis.dwd.de/werdis/start_js_JSP.do). Daily mean values of air temperature were taken from a weather station close to the Hainich site, that is Leinefelde (51°23′N, 10°18′E, altitude 356 m a.s.l.), for the period 1989–2007.

4 Results

Figure 1a depicts the vegetation phenology based on daily NDVI satellite observations. Figure 2a displays the time series of daily mean temperature for the same period. In the plots below, we show frequency components oscillating at different frequencies for both time series (Figs. 1b–e, 2b–e). The applied frequencies are marked by corresponding periods, i.e. by parts of the period length of one year.

For Germany, the hottest temperatures of the season are typically experienced in July. On average, NDVI data reach their maximum value on the 194th day of the year, whereas the highest temperature is measured on the 200th day of the year. Therefore, NDVI reaches its maximum already before the average daily temperature has peaked. Quantifying shifts in relation to the first day of the following year, this means that the maximum of average daily NDVI is $365 - 194 = 171$ days in advance, whereas the corresponding value of temperature is $365 - 200 = 165$ days in advance. As a consequence, each calculated phase shift as function of time is expected to fluctuate around its mean value. By means of the results for scale-dependent phase analysis of NDVI and temperature time series, we are able to quantify fluctuations in the timing of the seasons and phase shifts in relation to the normal annual rhythm (Fig. 3). Wavelet analysis shows how the phases evolve over time. The phase shifts are each indicated in days for time shift, i.e. shift in relation to the first day of the following year. On average, the phase of temperature has a smaller value for time shift than the phase of NDVI values at each period. Regarding the course of the year, however, events of satellite observations occur a few days earlier than temperature events, as expected for this case.

Another issue has to be considered when analyzing the relation between NDVI and temperature phases (Fig. 3). On closer inspection, a striking similarity between NDVI and temperature phase functions becomes apparent. Obviously, NDVI phases compared to temperature phases show these phases matched but shifted. The shifts seem to be constant in case of specific periods and outside of a zone affected by edge effects. Roughly speaking, the curves are phase locked between the years 1994 and 2003, whereas the first and the last five years are likely affected by edge effects. At first sight this seems to be in conflict with specifications given by Torrence and Compo (1998) for such intervals. According to the authors, the so-called cone of influence would span, for instance, approximately 1.4 years for Morlet wavelets of a one year period. The error caused by a discontinuity at the edge would drop by a factor e^{-2} within this cone. We would like to point out that in our case however, the analysis is carried out with repeated applications of wavelet transforms. The functions under consideration for phase analysis are influenced by edge effects themselves. Moreover, our method requires higher accuracy in calculation of wavelet transforms. Therefore, we expect a much longer interval. In order to study more precisely the influence of edge effects, this cone is assessed by means of simulated data. Seasonal phases of an undisturbed sinusoidal oscillation feature intervals where the function is not constant and thus visualize the region in which edge effects become noticeable (Fig. 3). The outcome of this is that the interval is 4–5 years. It is slightly different depending on for which function the phase is calculated. Functions of lower period have higher values for the amplitudes near the edges due to the discontinuities at the endpoints. Therefore, they transfer inflated values to the phase calculation and cause a longer range of edge effects than others. Figure 3 illustrates that, inside the cone of influence, oscillations may be out of phase. However, outside the cone of influence, phases can be found to occur time-delayed and one phase seems to be the delayed copy of the other one. Therefore, it is not enough to calculate phase differences in relation to the annual cycle. Instead, an additional study of phase locking over a longer period would be conducive.

In order to check whether the phase difference between seasonal phases of NDVI and temperature time series is constant over time, the results for the coherence phases computed for the 4–5½ year frequency band are presented

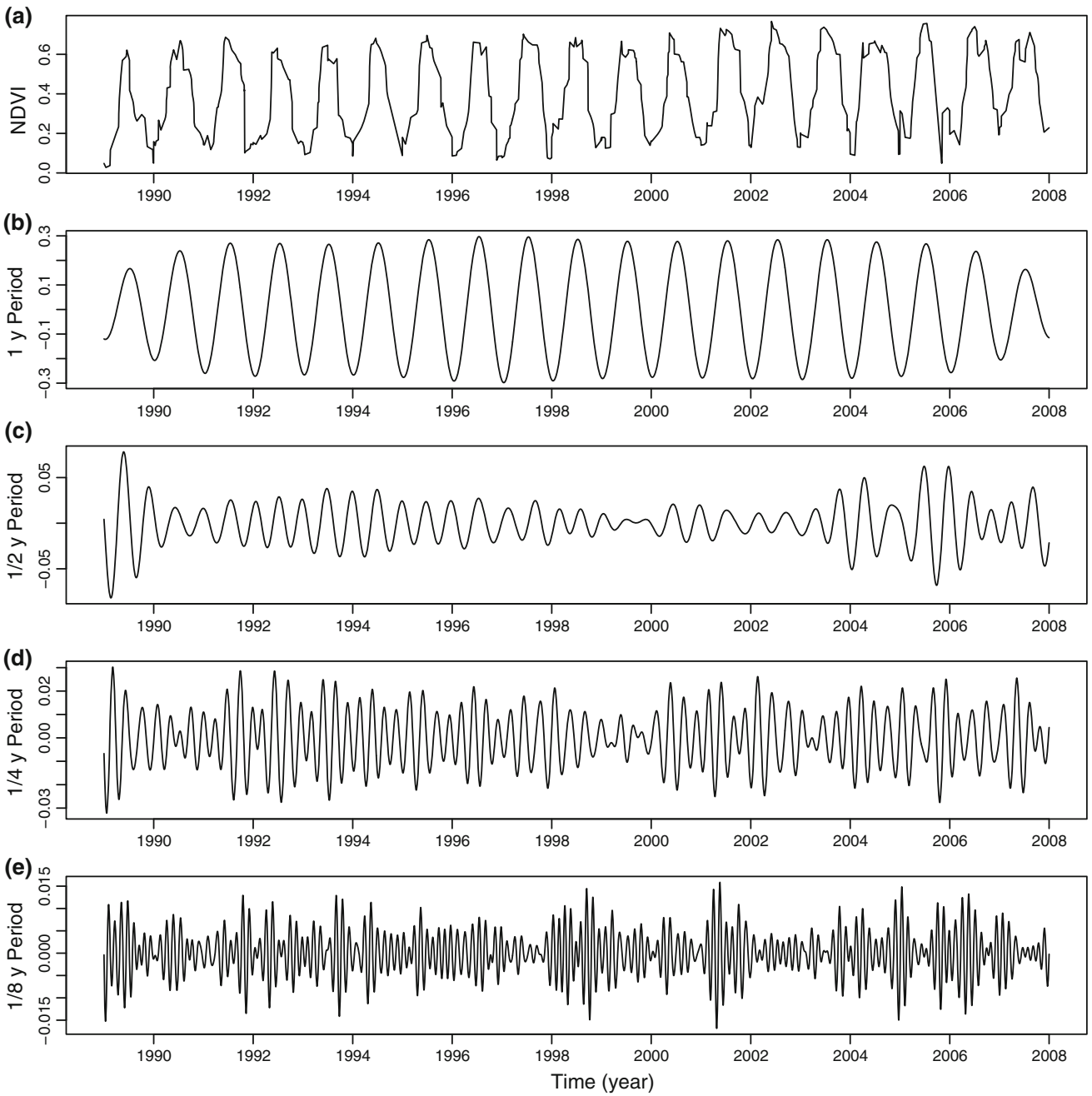

Fig. 1 **a** Time series of vegetation phenology based on daily NDVI satellite observations in the Hainich National Park, Thuringia, Germany. **b–e** Its components resulting from a time–frequency analysis of the normalized series at different periods, i.e., parts of the period length of one year

in Fig. 4. The analysis is based on deliberately shortened time series due to the edge effects. Obviously, at the one year period, phase locking does not exist. For seasonal phases, however, it becomes apparent that the phase difference is almost constant over time. The two time series appear to be phase-locked with a lag of approximately 300 days. This becomes most evident at the 1/8 year period. Therefore, in an effort to understand coherence of temperature and NDVI oscillations, a scale-dependent analysis seems to be relevant. To support this assumption, we additionally run a calculation ignoring the step where the time series are decomposed in frequency components and applying the two last steps of our method to the original time series. As expected for this case, the result indicates that there is no constant phase relationship between temperature and NDVI observations and that this approach is comparable to that of the one year period.

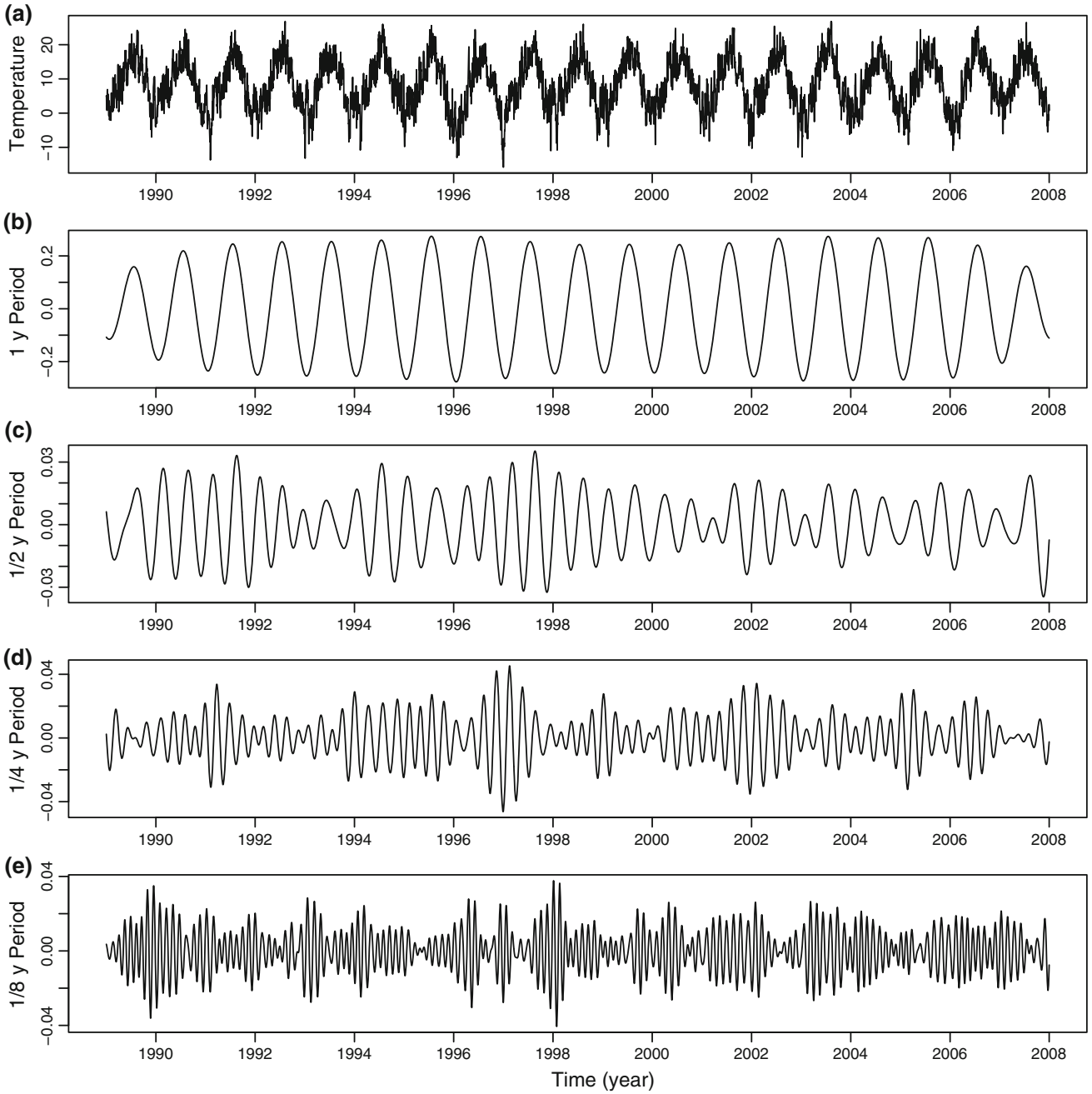

Fig. 2 **a** Time series of daily mean temperature data (°C) in Leinefelde, close to the Hainich National Park, Thuringia, Germany. **b–e** Its components resulting from a time–frequency analysis of the normalized series at different periods, i.e., parts of the period length of one year

In order to prove that this phase locking indeed exists at least at the 1/8 year period, the hypothesis that the phase differences $\Phi(\tau)$ presented in Fig. 4 can be regarded as constant over time should be confirmed or rejected in terms of scale. Therefore, we need to evaluate the strength of phase synchronization using an appropriate statistic. Allefeld and Kurths (2004) proved that the mean resultant length (MRL)

$$\mathrm{MRL} = \sqrt{\langle \cos(\Phi(\tau)) \rangle^2 + \langle \sin(\Phi(\tau)) \rangle^2},$$

where $< >$ is the temporal average, is a measure of the concentration of the underlying distribution. On the one hand, for oscillations of perfect phase synchronization, i.e. in case that their phase difference is constant over the whole time interval of interest, MRL is one. On the other hand, the MRL tends to zero for oscillations of increasingly asynchronous modifications and parts (Paluš and Novotná 2006). These characteristics can be utilized for statistical testing. For this purpose, the MRLs are calculated for both

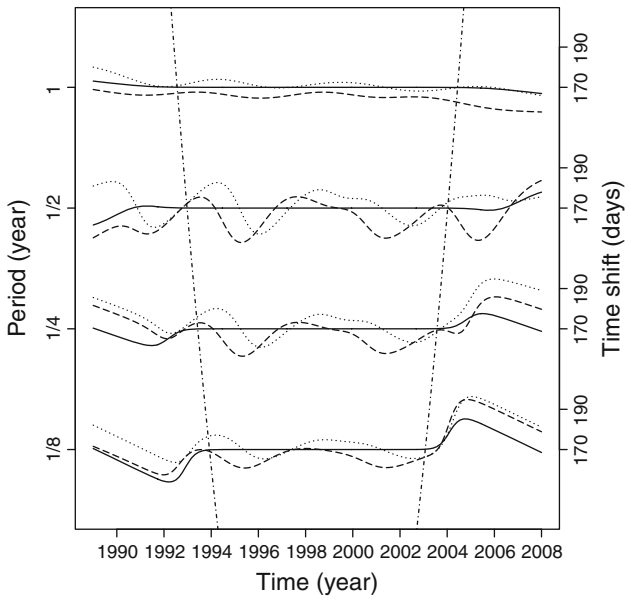

Fig. 3 Seasonal phases for NDVI data (*dotted lines*) and temperature data (*dashed lines*). Different components marked by different periods are used for both NDVI and temperature data. Phase shifts are indicated in days for time shift, i.e., days in forerun to the following year. Seasonal phases of simulated data of an undisturbed sinusoidal oscillation (*solid lines*) visualize the region in which edge effects become noticeable. The *dot–dashed lines* indicate this cone of influence

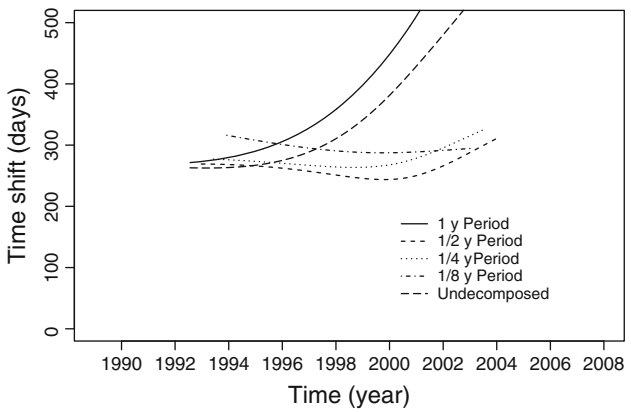

Fig. 4 Phase differences between seasonal phases of NDVI and temperature time series and, for comparison, phase difference between phases of the original undecomposed NDVI and temperature time series

phase differences of seasonal phases (Fig. 4) and phase differences of 1,000 sets of randomly generated data. For the latter ones, all phases must be randomly generated, whereas amplitudes, frequencies, and autocorrelations of original data need to be preserved (Paluš and Novotná 2011). Because, in general, the MRL for synchronized processes will be larger than for unsynchronized processes, the probability P of a random occurrence of MRL (randomly generated data) $\geq$ MRL(original data) should be smaller than 0.05. If so, the phase locking would be significant. The results for such probabilities P in terms of period are summarized in Table 1. Our findings confirm the hypothesis that phase locking exists at the 1/8 year period. Since the phase synchronization is significant only in case of the 1/8 year period, the results also indicate the importance of scale-dependent analyses.

5 Discussion

Morlet wavelets can serve as a helpful tool for decomposing time series with respect to time and period. Using such decompositions for a combined concept of phase and coherence analysis of bivariate time series, we are able to detect their inter-annual variations of phases and to decide whether there is any scale-dependent phase-locking. By applying this approach to temperature and NDVI time series, we are able to identify a coherent phase emerging at the 1/8 year period. It enables us to measure a time shift of about one year.

Our findings are supported by several authors indicating that, for deciduous trees, climate variables such as temperature influence the phenological timing of the following year. Obviously, this relationship is linked by photosynthetic processes as well as accumulation and depletion of carbohydrate reserves.

Gough et al. (2010) pointed out that thermal regulation of growing season length and duration of the photosynthetic period may have important consequences for the periodicity of seasonal tissue non-structural carbohydrates (NSC) cycles in temperate deciduous forests. They examined how shifts in accumulation of degree days relate to cycling processes of net primary production (NPP) and gross primary production (GPP) and how those relate to seasonal fluctuations in tissue NSC. In particular, they were able to demonstrate the coupling of temperature regulated carbon assimilation processes with temporal changes in NSC concentrations in aspens and oaks. Barbaroux and

Table 1 Statistical significance of the phase synchronization in terms of period

Period	*P* value
1 Year period	0.612
1/2 Year period	0.077
1/4 Year period	0.051
1/8 Year period	0.024*
Undecomposed	0.085

The results for P values of the MRL test statistic are listed for phase differences of seasonal phases (and, for comparison, phases of undecomposed time series)

A significance level of $P < 0.05$ is indicated with *asterisk*

Bréda (2002) examined seasonal fluctuations of NSC reserves (starch and soluble sugars), i.e. variations in NSC for beech and oak trees during a season. For beech, the study was carried out in a state forest in France (altitude 300 m). They observed a decrease in the concentration of sugars from March to June (i.e., until maximum leaf area index) and an increase in NSC concentration from June to October (i.e., until the start of leaf fall). Several studies revealed a relation between carbohydrate storage from the past year and growth in the present year in temperate deciduous forests. Especially for beech: Skomarkova et al. (2006) investigated the variability of radial growth int. al. in tree rings and analyzed the influence of climatic variables and carbohydrate storage on these parameters. They found, in particular, for the Hainich site in Germany that a certain part of the tree-ring width in a given year is explained by the growth conditions in the previous year. Moreover, Čufar et al. (2008) who studied beech trees at a typical forest site near Ljubljana, found tree-ring widths positive affected by the temperature of the previous November. This hypothesis is confirmed by Campioli et al. (2011). They investigated the same stand located in France as Barbaroux and Bréda (2002). The stand is composed of 90 % young beech. They showed that the air temperature of the previous year significantly correlates to the NPP–GPP ratio of wood and that lag effects between years play an important role. Since NPP and GPP relate to absorbed photosynthetically active radiation there is also a close relationship to remotely sensed NDVI profiles (Sjöström et al. 2011; Goward and Huemmrich 1992; Mariappan 2010).

Because most of the studies analyzed only individual beech trees over a short time span, there has been a need for a reliable and robust method to measure time lags between years. Moreover, there are no systematic investigations for answering the question: Which changes in the temperature regime at which time scales and for which shifts are the key drivers that strongly affect the growing season? Regarding these issues, our method is able to provide novel insight into the complex relationship between temperature and vegetation phenology of beech forests. Our method revealed that certain phase differences between temperature and NDVI observations are almost constant over time. It concerns mainly seasonal changes in temperature and NDVI cycle in respect of the normal annual rhythm.

6 Conclusion

Assessing the influence of drivers such as temperature on the phenological timings of plants requires the development of a method comparing phenological data and correlated drivers for different temporal shifts and at different time scales. We use Morlet wavelets to decompose signals into their frequency components. In addition, we calculate phase shifts of seasonal components in relation to the annual cycle and inter-annual phase differences of bivariate time series. Therefore, wavelet transforms provide a very appropriate tool to study the issue of periods when temperature has a potential influence on plant growing. As an example, vegetation phenology data based on satellite observations and appropriate temperature data are investigated. For a beech forest in the Hainich site in Germany, the two time series appear to be phase-locked with a time shift of approximately 300 days. In an effort to understand coherence of temperature and NDVI oscillations, we can first state that the more coherence is uniform, the more coupling between both signals is likely. Second, for the beech forest under consideration, this phase synchrony is significant at the 1/8 year period. Therefore, our study reveals that certain temperature fluctuations in relation to the normal annual cycle and arising during a 1–2 month period are likely coupled with phenological events in the following year. In particular, we support the assumption that a certain part of growing for beech trees is explained by the growth conditions in the previous year (Čufar et al. 2008; Skomarkova et al. 2006).

We believe that our analyses and results are promising for further studies of the influence of climatic drivers on the phenological timings of plants. Since identifying and quantifying of such interactions is a challenge, the method can be recommended for application to a wide range of bivariate time series of sufficient length and temporal resolution.

Acknowledgments We acknowledge support by the EU infrastructure project "Distributed Infrastructure for EXPErimentation in Ecosystem Research—EXPEER" (project reference 262060) funded under 7th Framework Programme. We would also like to thank Maximilian Lange (UFZ) who provided assistance with data assimilation.

References

Aguiar-Conraria A, Azevedo N, Soares M (2008) Using wavelets to decompose the time–frequency effects of monetary policy. Phys A 387:2863–2878

Allefeld C, Kurths J (2004) Testing for phase synchronization. Int J Bifurcat Chaos 14:405–416

Badeck F, Bondeau A, Böttcher K, Doktor D, Lucht W, Schaber J, Sitch S (2004) Responses of spring phenology to climate change. New Phytol 162:295–309

Barbaroux C, Bréda N (2002) Contrasting distribution and seasonal dynamics of carbohydrate reserves in stem wood of adult ring-porous sessile oak and diffuse-porous beech trees. Tree Physiol 22:1201–1210

Bunn A (2008) A dendrochronology program library in R (dplR). Dendrochronologia 26:115–124

Campioli M, Gielen B, Göckede M, Papale D, Bouriaud O, Granier A (2011) Temporal variability of the NPP–GPP ratio at seasonal

and interannual time scales in a temperate beech forest. Biogeosciences 8:2481–2492
Cazelles B, Stone L (2003) Detection of imperfect population synchrony in an uncertain world. J Anim Ecol 72:953–968
Cazelles B, Chavez M, McMichael A, Hales S (2005) Nonstationary influence of El Niño on the synchronous dengue epidemics in Thailand. PLoS Med 2:313–318
Cazelles B, Chavez M, Berteaux D, Ménard F, Vik J, Jenouvrier S, Stenseth N (2008) Wavelet analysis of ecological time series. Oecologia 156:287–304
Chmielewski F, Rötzer T (2001) Response of tree phenology to climate change across Europe. Agric For Meteorol 108:101–112
Cleland E, Chuine I, Menzel A, Mooney H, Schwartz M (2007) Shifting plant phenology in response to global change. Trends Ecol Evol 22:357–365
Čufar K, Prislan P, de Luis M, Gričar J (2008) Tree-ring variation, wood formation and phenology of beech (*Fagus sylvatica*) from a representative site in Slovenia, SE Central Europe. Trees 22:749–758
Delbart N, Picard G, Le Toan T, Kergoat L, Quegan S, Woodward I, Fedotova V (2008) Spring phenology in boreal Eurasia over a nearly century time scale. Glob Change Biol 14:603–614
Doktor D, Bondeau A, Koslowski D, Badeck F (2009) Influence of heterogeneous landscapes on computed green-up dates based on daily AVHRR NDVI observations. Remote Sens Environ 113:2618–2632
Foufoula-Georgiou E, Kumar P (1997) Wavelet analysis for geophysical applications. Rev Geophys 35(4):385–412
Gough CM, Flower CE, Vogel CS, Curtis PS (2010) Phenological and temperature controls on the temporal non-structural carbohydrate dynamics of *Populus grandidentata* and *Quercus rubra*. Forests 1:65–81
Goward S, Huemmrich K (1992) Vegetation canopy PAR absorptance and the normalized difference vegetation index: an assessment using the SAIL model. Remote Sens Environ 39:119–140
Grenfell B, Bjørnstad O, Kappey J (2001) Travelling waves and spatial hierarchies in measles epidemics. Nature 414:716–723
Hudson I (2010) Interdisciplinary approaches: towards new statistical methods for phenological studies. Clim Change 100:143–171
Hudson I, Keatley MR, Kang I (2011) Wavelet characterization of eucalypt flowering and the influence of climate. Environ Ecol Stat 18:513–533
Klvana I, Berteaux D, Cazelles B (2004) Porcupine feeding scars and climatic data show ecosystem effects of the solar cycle. Am Nat 164:283–297
Lachaux JP, Rodriguez E, le van Quyen M, Lutz A, Martinerie J, Varela F (2000) Studying single-trials of phase synchronous activity in the brain. Int J Bifurcat Chaos 10:2429–2439
Lu P, Yu Q, Liu J, He Q (2006) Effects of changes in spring temperature on flowering dates of woody plants across China. Bot Stud 47:153–161
Mariappan N (2010) Net primary productivity estimation of Eastern Ghats using multispectral MODIS data. Int J Geomat Geosci 1:406–413
Menzel A (2000) Trends in phenological phases in Europe between 1951 and 1996. Int J Biometeorol 44:76–81
Menzel A (2003) Plant phenological anomalies in Germany and their relation to air temperature and NAO. Clim Change 57:243–263
Menzel A, Sparks T, Estrella N, Roy D (2006) Altered geographic and temporal variability in phenology in response to climate change. Glob Ecol Biogeogr 15:498–504
Miller-Rushing A, Inouye D, Primack R (2008) How well do first flowering dates measure plant responses to climate change? The effects of population size and sampling frequency. J Ecol 96:1289–1296
Paluš M, Novotná D (2006) Quasi-biennial oscillations extracted from the monthly NAO index and temperature records are phase-synchronized. Nonlin Process Geophys 13:287–296
Paluš M, Novotná D (2011) Northern hemisphere patterns of phase coherence between solar/geomagnetic activity and NCEP/NCAR and ERA40 near-surface air temperature in period 7–8 y oscillatorymodes. Nonlin Process Geophys 18:251–260
Paluš M, Novotná D, Tichavský P (2005) Shifts of seasons at the European mid-latitudes: natural fluctuations correlated with the North Atlantic oscillation. Geophys Res Lett 32:L12805
Parmesan C (2007) Influences of species, latitudes and methodologies on estimates of phenological response to global warming. Glob Change Biol 13:1860–1872
Percival D, Walden A (2000) Wavelet methods for time series analysis. Cambridge University Press, Cambridge
Percival D, Wang M, Overland J (2004) An introduction to wavelet analysis with applications to vegetation time series. Community Ecol 5:19–30
Pikovsky A, Rosenblum M, Kurths J (2001) Synchronization, a universal concept in nonlinear sciences. Cambridge University Press, Cambridge
Post E, Pedersen C, Wilmers C, Forchhammer M (2008) Phenological sequences reveal aggregate life history response to climatic warming. Ecology 89:363–370
Sjöström M, Ardö J, Arneth A, Boulain N, Cappelaere B, Eklundh L, Veenendaal E (2011) Exploring the potential of MODIS EVI for modeling gross primary production across African ecosystems. Remote Sens Environ 115:1081–1089
Skomarkova MV, Vaganov EA, Mund M, Knohl A, Linke P, Boerner A, Schulze ED (2006) Inter-annual and seasonal variability of radial growth, wood density and carbon isotope ratios in tree rings of beech (*Fagus sylvatica*) growing in Germany and Italy. Trees 20:571–586
Sparks T, Jeffree E, Jeffree C (2000) An examination of the relationship between flowering times and temperature at the national scale using long-term phenological records from the UK. Int J Biometeorol 44:82–87
R Development Core Team (2010) R: a language and environment for statistical computing. R Foundation for Statistical Computing, Vienna. ISBN 3-900051-07-0. http://www.R-project.org}
Torrence C, Compo G (1998) A practical guide to wavelet analysis. Bull Am Meteorol Soc 79:61–78
Torrence C, Webster P (1999) Interdecadal changes in the ENSO–monsoon system. J Clim 12:2679–2690
Wareing P (1953) Growth studies in woody species V. Photoperiodism in dormant buds of *Fagus sylvatica* L. Physiol Plant 6:692–706. doi:10.1111/j.1399-3054.1953.tb08442.x
White M, Brunsell N, Schwartz M (2003) Vegetation phenology in global change studies. In: Schwartz M (ed) Phenology: an integrative environmental science. Kluwer Academic Publishers, Dordrecht, pp 453–466
Yang T, Xu C, Shao Q, Chen X, Lu G, Hao Z (2010) Temporal and spatial patterns of low-flow changes in the Yellow River in the last half century. Stoch Environ Res Risk Assess 24:297–309
Yang Y, Xu J, Hong Y, Lv G (2012) The dynamic of vegetation coverage and its response to climate factors in Inner Mongolia, China. Stoch Environ Res Risk Assess 26:357–373
Zhang Q, Xu C, Chen Y (2010) Wavelet-based characterization of water level behaviors in the Pearl River estuary, China. Stoch Environ Res Risk Assess 24:81–92